Earthquake Geotechnical Engineering for Protection and Development of Environment and Constructions – Silvestri & Moraci (Eds)
© 2019 Associazione Geotecnica Italiana, Rome, Italy, ISBN 978-0-367-14328-2

Modeling the cyclic softening of a mildly sensitive clay

M. Kiernan & J. Montgomery
Auburn University, Auburn, AL, USA

ABSTRACT: This paper examines the use of a recently developed bounding surface plasticity model (PM4Silt) to capture the cyclic softening behavior of a mildly sensitive clay. The constitutive model has been developed to model the cyclic behavior of fine-grained soils and modified in this study to model the structural degradation of a sensitive soil. Model calibration and single-element simulation results for monotonic and cyclic loading are presented. The calibrated model is then used to simulate the Fourth Avenue landslide from Anchorage, Alaska, USA, which has been attributed to cyclic softening in the sensitive clay foundation during the 1964 Great Alaska Earthquake. Results from numerical simulations are compared with observed displacements and the sensitivity of the solution to the calibration procedure and the mesh size is explored.

1 INTRODUCTION

Strain-softening of fine-grained soils has contributed to significant infrastructure damage in past earthquakes (e.g., Shannon & Wilson 1964, Heritage 2013, Nakamura et al. 2014). The potential impacts from seismically-induced displacements are increasingly being analyzed using nonlinear deformation analyses (NDAs). The reliability of results from NDAs depends in part on using constitutive models that can represent the aspects of soil behavior pertinent to the specific problem being modeled. Few validated constitutive models are publicly available that can analyze potential deformations from cyclic softening of clayey soils. This stands in contrast to the large number of constitutive models that are available to practicing engineers to estimate potential liquefaction-induced deformations in granular deposits.

The undrained response of clays is often modeled in NDAs using a single value of undrained shear strength. The validity of this approach is questionable for clays that are prone to strain softening. Modeling strain-softening first requires a constitutive model that can account for strength loss. A compromise must be then be made be made between model simplicity and its ability to accurately represent complex soil behavior. Total-stress based models exist (Andersen & Jostad 2005, Beaty & Dickenson 2015) which often employ a simplified formulation of stress-stress strain response and do not address coupling between the soil and pore fluid (Taibet et al. 2011). More complex effective-stress based models also exist which consider soil and pore fluid individually and are often grounded in critical state theory (e.g., Park 2011, Seidalinov & Taibet 2014, Boulanger & Ziotopoulou 2018). A common limitation of both model types is the ability to represent strain localization during softening. In numerical simulations strains may localize over a single row of elements resulting in a mesh dependent solution.

The current study uses the recently published PM4Silt constitutive model (Boulanger & Ziotopoulou 2018). PM4Silt is a critical state compatible effective stress based bounding surface plasticity model formulated to model the cyclic response of low plasticity fine grained soils. This study introduces a modification to PM4Silt, which helps better capture the response of mildly sensitive clays by accounting for the effects of structural degradation on the critical state line. The modified model is first calibrated using single element simulations and then used to simulate the Fourth Avenue landslide, which failed during the 1964 Great Alaska Earthquake. The influence of the constitutive model parameters on the simulation results is explored. Potential limitations of the proposed approach and possible future improvements are discussed.

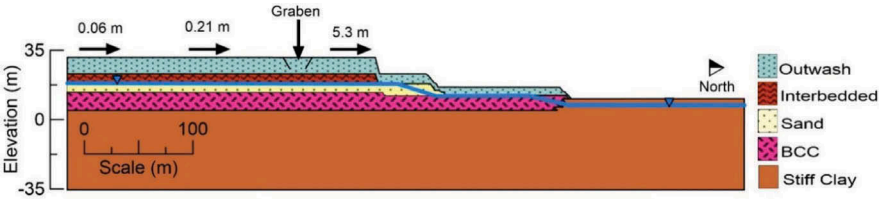

Figure 1. Fourth Avenue cross-section with observed deformations (after Shannon & Wilson 1964)

2 FOURTH AVENUE LANDSLIDE

The Fourth Avenue landslide was initiated by the 1964 Great Alaska Earthquake on March 27th, 1964. The magnitude 9.2 earthquake was caused by the rupture of a subduction zone interface near Prince William Sound (Ichinose et al. 2007). No ground motion recordings exist for this event, but witness descriptions and observed damage patterns indicate peak ground acceleration of up to about 0.2g with 2 to 3 minutes of strong shaking in the Anchorage area (Moriwaki 1985). Ground failures due to shaking were extensive in the Anchorage area and many were attributed to strain-softening of the sensitive Bootlegger Cove Clay (BCC) deposit (Hanson 1965, Woodward-Clyde 1982, Idriss 1985). Of the numerous ground failures that occurred during the earthquake the Fourth Avenue landslide was selected for this numerical evaluation because of the well-defined failure mechanism and the numerous site characterization studies performed by previous researchers near the site. Figure 1 presents an idealized cross-section of the Fourth Avenue landslide with observed deformations as approximated from site characterizations published by Shannon & Wilson (1964).

3 SITE INVESTIGATIONS AND SOIL PROPERTIES

Site stratigraphy and strength characteristics for the Fourth Avenue slide were estimated from index tests and standard penetration tests (SPTs) performed by Shannon & Wilson (1964) along with cone penetration tests (CPTs), direct shear (DS), direct simple shear tests (DSS), triaxial tests, and miniature vane shear tests performed by Woodward-Clyde (1982). A shear wave velocity profile was estimated from nearby downhole test performed by Nath et al. (1997).

The peak undrained shear strength ratio ($S_{u,pk}/\sigma'_v$) for the critical BCC layer was calculated from the relationship provided by Woodward-Clyde (1982) which was derived from DSS tests (equation 1). Woodward-Clyde (1982) reported a mean *OCR* of 1.3 for the BCC. Using an *OCR* of 1.3, the value of $S_{u,pk}/\sigma'_v$ used in this study was calculated to be 0.23. The term sensitivity (S_t) describes the amount of strength loss expected for a strain softening material and is defined as the ratio of peak undrained shear strength to remolded undrained shear strength. Idriss (1985) reported sensitivities ranging from 2 to 11 with an average sensitivity of 3.3 based on miniature vane shear test, CPTs, and DS tests. Stark & Contreras (1998) report a sensitivity near 4 for the BCC in the slide area based on constant volume ring shear tests. This paper uses a BCC sensitivity of 4 for the baseline simulations with a shear wave velocity of 220 m/s (after Nath et al. 1997).

$$\frac{S_{u,pk}}{\sigma'_v} = 0.185(OCR)^{0.78} \tag{1}$$

The interbedded and stiff clay layers were estimated to have $S_{u,pk}/\sigma'_v$ values ranging from about 0.20 to 0.55 based on CPTs and DSS tests. Based on this data, a $S_{u,pk}/\sigma'_v$ value of 0.35 was used in this study for both the interbedded and stiff clay layers. The shear wave velocities for the interbedded and stiff clay layers were estimated to be 300 m/s and 450 m/s, respectively (Nath et al. 1997). The strength characteristics of the coarse-grained soils were estimated from SPTs performed by Shannon & Wilson (1964) in the form of $(N_1)_{60}$ values. The sand and outwash

Table 1. Summary of Selected Input Motions

Earthquake Name	Station ID	CH	Mw	Epicentral Distance (km)	Scale Factor	PGA of Scaled Motion (g)	Arias Intensity (m/s)	V_{S30} (m/s)
Chile 2/27/2010	CUR	NS	8.8	171	0.60	0.28	3.8	525
		EW			0.55	0.23	3.3	
	HUA	L	8.8	136	0.43	0.16	1.4	530
		T			0.43	0.19	1.6	
	LLO	L	8.8	274	0.50	0.22	1.2	370
		T			0.40	0.16	1.6	
	TAL	L	8.8	113	0.70	0.33	5.6	550
		T			0.60	0.25	3.9	
Japan 3/11/2011	FKS 015	NS	9.0	227	1.25	0.35	2.5	696
		EW			1.0	0.22	1.4	
	TCG 001	EW	9.0	253	0.70	0.20	1.2	580
		EW			0.70	0.29	1.8	

layers were estimated to have average $(N_1)_{60}$ values of about 45 and 50, respectively. A shear wave velocity of 300 m/s was estimated for both the sand and outwash layers (Nath et al. 1997).

4 NUMERICAL SIMULATIONS

The commercial finite difference code FLAC (v8.0, Itasca 2016) was used to perform 2D plane strain simulations. Pre-earthquake stresses were established using a fixed base and roller boundaries along the sides. During this stage, the zones were assigned an elastic, perfectly plastic Mohr-Coulomb constitutive model with stiffness and drained strength parameters identical to those used in the dynamic phase (described below). During dynamic loading. free-field boundaries are applied at the model sides with a compliant boundary along the base. Details on the formulation and implementation of these boundary conditions are given by Itasca (2016).

No strong motion recordings exist from the 1964 Alaska quake, so input motions from the 2010 Chile and 2011 Japan subduction quakes were used instead. The processed Chile records and raw Japan records were downloaded from CESMD (2018). The Japan motions were processed according to Ancheta et al. (2013). Each horizontal component was treated as an individual motion, leading to 12 total time histories. The horizontal motions were linearly scaled to match the target spectrum for the site (Beaty & Dickenson 2015), over periods of approximately 0.6 to 1.0 seconds, which roughly encompasses the low strain period of the site. The same scaling factor was applied to the vertical component of the motion. Each of the selected motions was applied at the compliant boundary as a stress time history (Itasca 2016). A summary of the selected motions is shown in Table 1.

5 CONSTITUIVE MODELS FOR DYNAMIC LOADING

The dynamic response of the sand and outwash layers are modeled using PM4Sand (Boulanger & Ziotopoulou 2017). PM4Sand is a critical state compatible, effective stress-based, bounding surface plasticity model used to model cyclic liquefaction in granular soils. Calibration of PM4Sand was performed by first setting the relative density for each layer based on the estimated $(N_1)_{60}$ values. The shear modulus coefficients (G_o) were set to achieve the desired shear wave velocities. The h_o parameter was adjusted so that the cyclic modulus reduction behavior for sands matched the curves provided by EPRI (1993) at the appropriate layer depths. The h_{po} parameter was finally adjusted to achieve the desired to cyclic stress ratio (CSR) to cause 3% strain in 15 uniform loading cycles. The target CSR value was capped at 0.8 based on the relationships provided in Idriss & Boulanger (2010) for the estimated $(N_1)_{60}$ values.

Table 2. Summary of constitutive model input parameters

Layer	$S_{u,cs,eq}/\sigma'_v$	$n^{b,wet}$	h_o	h_{po}	G_o	$(N_1)_{60}$
Stiff Clay	0.35	0.8	1.6	2.5	1211	N/A
Interbedded	0.35	0.8	1.7	2	1303	N/A
Sand	N/A	N/A	0.65	0.034	1177	50
Outwash	N/A	N/A	0.62	0.012	2000	45

The dynamic response of the stiff clay, interbedded zone and BCC layers were modeled using PM4Silt. PM4Silt utilizes the framework of PM4Sand but is adapted to better represent the cyclic response of silts and clays as opposed to granular soils. Calibration of PM4Silt was performed by first setting the undrained shear strength at critical state ($S_{u,cs,eq}/\sigma'_v$) to the estimated values. The shear modulus coefficients (G_o) were set to achieve the desired shear wave velocities. The contraction rate parameter (h_{po}) was then adjusted, so that the CSR required to cause 3% shear strain in 30 uniform loadings was equal to 60% of $S_{u,cs,eq}/\sigma'_v$. All calibrations were performed using single element DSS drivers with σ'_v =100 kPa. Final calibration parameters for the non-BCC layers are summarized in Table 2. Calibration of the BCC layer will be discussed in the next section.

6 MODIFICATION OF PM4SILT

PM4Silt is a critical state-compatible model, which means that the final undrained strength of the soil is determined by the initial void ratio (e_o) of the clay and the position of the critical state line (CSL) (Boulanger & Ziotopoulou 2017). Within the model, the position of the CSL is set by $S_{u,cs,eq}/\sigma'_v$ and the peak strength is set by adjusting the calibration parameter $n^{b,wet}$. For insensitive clays, this approach works well, but for sensitive clays the difference between the peak and remolded strength may be large and this calibration process becomes difficult. To overcome this, the PM4Silt model was modified to allow the position of the CSL (defined through the intercept Γ) to move during shearing to represent progressive structural degradation of the sensitive BCC toward a residual limit (Figure 2a). This is conceptually similar to the movement of the normal compression line, which has been observed in sensitive clays (e.g., Yong & Nagaraji 1977). In the modified version of the model, the critical state line moves towards the remolded position with increasing plastic shear strain (Figure 2b). The softening process only occurs when the incremental stiffness (i.e., the change in shear stress divided by the change in shear strain) is negative. The modification introduces two additional input parameters. The first is the residual undrained shear strength ratio ($S_{u,res}/\sigma'_v$) which is determined by dividing the peak undrained shear strength ratio ($S_{u,pk}/\sigma'_v$) by the soil sensitivity (S_t). The second additional input parameter is the remolding strain (γ_{rem}), which controls the interval of strain over which softening occurs.

The modified PM4Silt model required a slightly revised calibration procedure for the critical BCC layer than described above. All model calibrations were performed using single element DSS drivers with a vertical consolidation stress of 100 kPa as recommended by Boulanger & Ziotopoulou (2017). The parameter G_o was set to 420 to achieve the desired shear wave velocity of

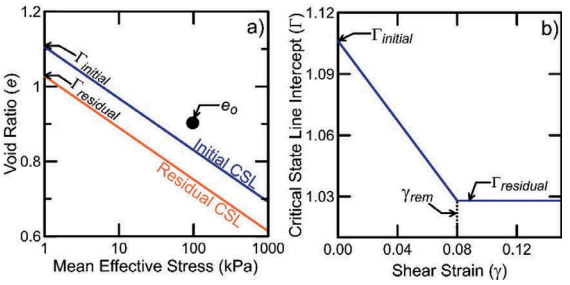

Figure 2. Schematic illustrating the strain softening process in the modified PM4Silt model.

Table 3. Final calibrated BCC input parameters

S_t	Softening Rate	$S_{u,res}/\sigma'_v$	$\Gamma_{initial}$	$\Gamma_{residual}$	γ_{rem}	$n^{b,wet}$	h_o	h_{po}
3	Fast	0.075	1.1063	1.0588	0.04	0.65	0.3	17
4	Slow	0.056	1.1063	1.0438	0.08	0.65	0.3	17
*4	Fast	0.056	1.1063	1.0438	0.04	0.65	0.3	17
5	Fast	0.045	1.1063	1.0265	0.04	0.65	0.3	17

* Baseline Calibration

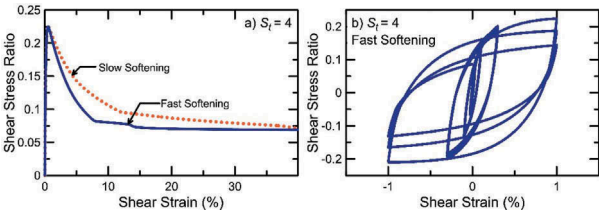

Figure 3. Undrained (a) monotonic and (b) cyclic DSS simulation results for a sensitivity of 4.

220 m/s. The remolded shear strength is specified through the remolded position of the critical state line (Fig. 2). The parameters $n^{b,wet}$ and initial position of the CSL ($\Gamma_{initial}$) are then iteratively adjusted to achieve the desired peak strength using a monotonic DSS driver. The parameter γ_{rem} is then adjusted to change the rate of softening. The parameter h_o was then set to match the modulus reduction curves provided by Vucetic & Dobry (1991) for clays with a PI near 15. The contraction rate parameter (h_{po}) was set last, to achieve the desired cyclic strength (3% strain in 30 cycles with a cyclic stress ratio equal to 50% of $S_{u,pk}/\sigma'_v$). Final input parameters for all BCC calibrations are shown in Table 3. Figure 3 illustrates the calibrated model behavior in undrained monotonic and cyclic DSS simulations for a sensitivity of 4 and two different rates of softening.

7 RESULTS AND DISCUSION

The baseline simulations for the Fourth Avenue landslide used S_t = 4 and the faster softening rate, along with the HUA-T motion. Lateral displacement contours for the baseline case are shown in Figure 4. Deformation patterns and magnitudes are comparable to those observed at the Fourth Avenue site, including a well-defined translational failure mechanism and a failure plane that intercepts the ground surface just behind the crest of the slope. Shear strains remained roughly horizontal in the BCC until they propagated up to the bluff behind the upper crest. Pressure ridges can be seen at the toe consistent with observations. The deformation patterns are consistent with those observed by Kiernan & Montgomery (2018) using a strain-softening Mohr-Coulomb model, although they had to use a higher sensitivity value to obtain comparable displacements.

7.1 *Effect of input motion*

The effect of input motion was studied by repeating the baseline analyses with several input motions. Deformation patterns were similar to those shown in Figure 4 across the suite of

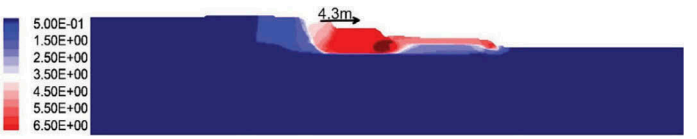

Figure 4. Lateral displacement contours for baseline simulation (zero contour omitted)

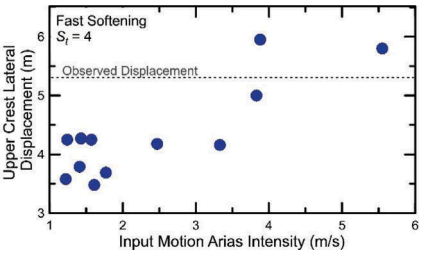

Figure 5. Upper crest displacement versus Arias intensity for selected motions

motions, but deformation magnitudes generally increased with Arias intensity (Figure 5). This increase in displacement with Arias Intensity is consistent with trends shown by previous studies (e.g., Travasarou et al. 2003). A similar trend would likely be observed for other ground motion parameter that incorporate both magnitude and duration, such as the destructiveness potential factor (Araya & Saragoni 1984). The HUA-T motion produces approximately median displacements among the chosen records and is used for the remaining simulations.

7.2 *Effect of BCC sensitivity and softening rate*

The effect of the BCC sensitivity was examined by repeating the baseline analysis with a sensitivity of 3 and 5. The effect of increasing the BCC sensitivity on the upper crest lateral displacement is illustrated in Figure 6a. The BCC begins to soften in all three simulations after approximately 35 seconds of shaking, which is where the peak acceleration occurs in the HUA-T motion. The simulation with sensitivity of 3 showed an upper crest lateral displacement of less than half the observed value. The simulation with a sensitivity of 5 was halted before the end of shaking due to excessive mesh deformation. Simulations with the proposed model and a sensitivity between 4 and 5 would likely produce deformations consistent with site observations. This range of sensitivities is slightly higher than the mean BCC sensitivities reported by previous authors (Idriss 1985, Stark & Contreras 1998), but well within the range of measured values.

The effect of the BCC softening rate was examined by repeating the baseline analysis with a softening rate that was approximately half as fast as the baseline simulation (Figure 6b). The results show that large displacements begin to occur at the same point in the record for both softening rates. The two simulations also reach a similar final displacement value, although the slower softening rate requires significantly more shaking to reach this value. These results indicate that the softening rate does not appear to have a major effect on final deformation magnitudes if the material is able to fully soften during shaking. This is expected as the final deformed shape will be controlled more by the remolded strength (and therefore the sensitivity) than the softening rate.

7.3 *Effect of mesh density*

The effect of mesh density was examined by repeating the baseline analysis with a finer and coarser mesh. All previous analyses utilized a mesh with 14,602 zones with a maximum BCC

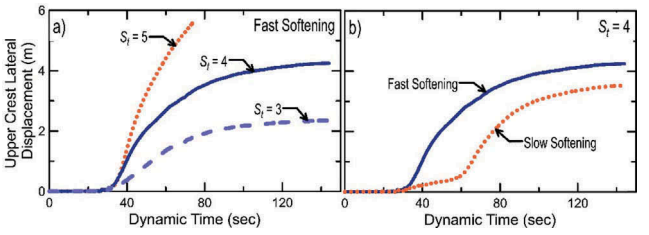

Figure 6. Effect of (a) BCC sensitivity and (b) softening rate on upper crest displacement.

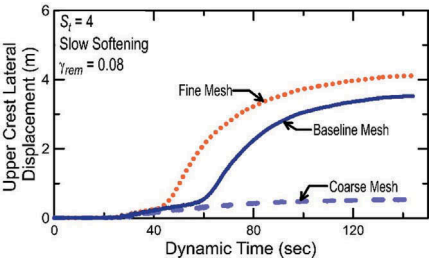

Figure 7. Time histories of upper crest displacement for varying mesh densities.

zone height of 1.3m. A coarser mesh (7,425 zones) and finer mesh (24,298 zones) with maximum BCC zones heights of 1.8m and 0.9m, respectively, were used to examine the effects of mesh size on the results. The BCC calibration for $S_t = 4$ and the slower softening rate are used in the following simulations to ensure that the fine mesh models are not halted due to geometry errors. Figure 7 illustrates the effect of mesh density on the modified PM4Silt model. All three meshes show displacements beginning to increase after approximately 35 seconds of shaking. The fine mesh then shows the fastest increase in displacement, while the coarse mesh only shows a slight increase of displacement with time. The final displacements of the fine and medium meshes are similar although the softening rate is different. This result is expected, as the smaller zones will experience larger strains, and therefore faster softening, for a given magnitude of displacement. These results indicate that the solution is mesh dependent and a regularization scheme to reduce this dependence would be beneficial. The authors are currently implementing a softening scaling approach similar to the one used by Kiernan & Montgomery (2018) to address this.

8 SUMMARY AND CONCLUSIONS

A proposed modification to the existing PM4Silt constitutive model was used to simulate the Fourth Avenue landslide which failed during the 1964 Great Alaska Earthquake. The proposed modification softens the critical state line to a remolded state to replicate structural degradation in the sensitive BCC. The modification was shown capable of reproducing element level softening behavior in monotonic and cyclic loading in single element DSS drivers. The modification was also shown capable of reproducing system level cyclic softening behavior in full scale simulations of the Fourth Avenue landslide. Deformation patterns and displacement magnitudes observed at the Fourth Avenue site using simulations with the modified PM4Silt model were in reasonable agreement with observations. The softening rate of the BCC did affect the rate of displacement increase but did not significantly affect the final displacement because the duration of loading was sufficient to remold the clay. Mesh dependency of the solution was observed and was most significant for the coarsest mesh, which was not able to fully soften under the imposed displacements. Implementation of a regularization technique may be able to address this issue and remains an area for future work. Simulations using additional case histories and lab test are needed to further validate the modified PM4Silt model and identify areas where improvements are needed.

REFERENCES

Ancheta, T. D., Darragh, R. B., Stewart, J. P., Seyhan, E., Silva, W. J., Chiou, B. S. J., Wooddell, K. E., Graves, R. W., Kottke, A. R., Boore, D. M., Kishida, T., & Donahue, J. L. (2013). PEER NGA-WEST2 Database. PEER Report 2013/03, Pacific Engineering Research Center, Univ. of California Berkeley.

Andresen, L. & Jostad, H. P. (2005). ANISOFT – Constitutive Model for Undrained Loading of Anisotropic and Strain-Softening Clay. *Geo-Frontiers Congress 2005*, Austin, Texas.

Araya, R. & Saragoni, G.R. (1984). Earthquake Accelerogram Destructiveness Potential Factor. *Proc. 8th World Conference on Earthquake Engineering 1984*. San Francisco, CA

Beaty, M. H. & Dickenson, S. E. (2015). Numerical Analysis for Seismically-Induced Deformations in Strain-Softening Plastic Soils. *Proc. 6th Intern. Conference on Earthquake Geotechnical Engineering*, Chirstchurch, NZ.

Boulanger, R. W. & Ziotopoulou, K. (2017). PM4Sand (version 3.1): A sand plasticity model for earthquake engineering applications. *Report No. UCD/CGM-17/01*, Center for Geotechnical Modeling, Department of Civil and Environmental Engineering, University of California, Davis, CA, March, 112 pp.

Boulanger, R. W. & Ziotopoulou, K. (2018). PM4Silt (Version 1): A silt plasticity model for earthquake engineering applications. *Report No. UCD/CGM-18/01*, Center for Geotechnical Modeling, Department of Civil and Environmental Engineering, University of California, Davis, CA.

Center for Eng. Strong Motion Data (CESMD) (2018). *http://www.strongmotioncenter.org/*

EPRI (1993). Electric Power Research Institute. Guidelines for site specific ground motions. *Rept. TR-102293*, 1–5, Pala Alto, California.

Hanson, W. (1965). Effects of the Earthquake of March 27, 1964, at Anchorage Alaska. *USGS Prof. Paper 542-A*.

Heritage, R. J. (2013). Cyclic softening case study: Wendover Retirement Village. *Proc. 19th NZGS Geotechnical Symposium*, Christchurch, Queensland.

Ichinose, G., Somerville, P., Thio, H. K., Graves, R., & O'Connell, D. (2007). "Rupture process of the 1964 Prince William Sound, Alaska, earthquake from the combined inversion of seismic, tsunami, and geodetic data." *Journal of Geophysical Research*, 112(B7)

Idriss, I. M. (1985). Evaluating Seismic Risk in Engineering Practice. *Proc. 11th Int. Conf. on Soil Mech. and Found. Eng.*, San Francisco, CA. 255–320.

Idriss, I. M. & Boulanger, R. W. (2010). SPT-based liquefaction triggering procedures. *Report UCD/CGM-10/02*, Department of Civil and Environmental Engineering, University of California,Davis, CA, 259 pp.

Itasca (2016). FLAC, Fast Lagrangian Analysis of Continua, Version 8.0. Itasca Consulting Group, Minneapolis, MN, 2017.

Kiernan, M. & Montgomery, J. (2018). Numerical Simulations of the Fourth Avenue Landslide Considering Strain Softening. *Proc. Geotechnical Earthquake Engineering and Soil Dynamics V*, Austin, TX, June 10-13th, 2018.

Moriwaki, Y., Vicente,E. E., Lai, S. S., & Moses, T. L. (1985). A Reevaluation of the 1964 "L" Street Slide. Final Report, State of Alaska, Department of Transportation and Public Facilities.

Nakamura, S., Wakai, A., Umemura, J., Sugimoto, H., & Takeshi, T. (2014). Earthquake induced landslides: Distribution, motion and mechanisms. *Soils and Foundations*, 54(4), 544–559.

Nath, S. K., Chatterjee, D., Biswas, N. N., Dravinski, M., Cole, D. A., Papageorgiou, A., Rodriguez, J. A., & Poran, C. J. (1997). Correlation Study of Shear Wave Velocity in Near Surface Geological Formations in Anchorage, Alaska. *Earthquake Spectra*, 13(1), 55–75.

Park, D. S. (2011). Strength Loss and Softening of Sensitive Clay Slopes. *Doctoral Dissertation*. University of California, Davis.

Shannon & Wilson (1964). Report on Anchorage area soil studies. *Rep. to USACE District, Anchorage, Alaska*. Contract no. DA-95-507-CIVENG–64–18.

Seidalinov, G. & Taiebat, M. (2014). Bounding surface SANICLAY plasticity model for cyclic clay behavior. *International Journal for Numerical and Analytical Methods in Geomechanics*, 38: 702–724. doi:10.1002/nag.2229

Stark, T. D. & Contreras, I. A. (1998). Fourth Avenue Landslide during 1964 Alaskan Earthquake. *Journal of Geotechnical and Geoenvironmental Engineering*, 124(2), 99–109.

Taiebat, M., Kaynia, A. M., & Dafalias, Y. F. (2011). Application of an Anisotropic Constitutive Model for Structured Clay to Seismic Slope Stability. *Journal of Geotechnical and Geoenvironmental Engineering*, 137(5), 492–504.

Travasarou, T., Bray, J. D., & Abrahamson, N. (2003). Empirical attenuation relationship for Arias Intensity. *Earthquake Engineering & Structural Dynamics*, 32(7),1133–1155.

Vucetic, M. & Dobry, R. (1991). Effect of soil plasticity on cyclic response. *Journal of Geotechnical Engineering*, 117(1), 89–107.

Woodward-Clyde Consultants (1982). Anchorage Office Complex, Geotechnical Investigation, Anchorage, Alaska. *Report to Alaska DOT and Public Facilities, Design and Construction, Anchorage, Alaska*.

Yong, R.N. & Nagaraj, T.S. 1977. Investigation of fabric and compressibility of a sensitive clay. *In Proceedings of the International Symposium on Soft Clay*, Asian Institute of Technology, pp. 327–333.